Neuro-Oncology Advances

6(1), vdae021, 2024 | https://doi.org/10.1093/noajnl/vdae021 | Advance Access date 9 February 2024

Discrimination of benign, atypical, and malignant peripheral nerve sheath tumors in neurofibromatosis type 1 using diffusion-weighted MRI

Inka Ristow, Michael G. Kaul, Maria Stark, Antonia Zapf, Christoph Riedel, Alexander Lenz, Victor F. Mautner, Said Farschtschi, Ivayla Apostolova, Gerhard Adam, Peter Bannas, Johannes Salamon†, and Lennart Well†,

All author affiliations are listed at the end of the article

Corresponding Author: Inka Ristow, MD, Department of Diagnostic and Interventional Radiology and Nuclear Medicine, University Medical Center Hamburg-Eppendorf, Martinistraße 52, 20246 Hamburg, Germany (i.ristow@uke.de).

†These authors contributed equally to this work and share senior authorship.

Abstract

Background. Neurofibromatosis type 1 (NF1) is associated with the development of benign (BPNST) and malignant (MPNST) peripheral nerve sheath tumors. Recently described atypical neurofibromas (ANF) are considered pre-malignant precursor lesions to MPNSTs. Previous studies indicate that diffusion-weighted magnetic resonance imaging (DW-MRI) can reliably discriminate MPNSTs from BPNSTs. We therefore investigated the diagnostic accuracy of DW-MRI for the discrimination of benign, atypical, and malignant peripheral nerve sheath tumors.

Methods. In this prospective explorative single-center phase II diagnostic study, 44 NF1 patients (23 male; 30.1 ± 11.8 years) underwent DW-MRI (*b*-values 0–800 s/mm^2) at 3T. Two radiologists independently assessed mean and minimum apparent diffusion coefficients ($ADC_{mean/min}$) in areas of largest tumor diameters and ADC_{dark} in areas of lowest signal intensity by manual contouring of the tumor margins of 60 BPNSTs, 13 ANFs, and 21 MPNSTs. Follow-up of ≥ 24 months (BPNSTs) or histopathological evaluation (ANFs + MPNSTs) served as diagnostic reference standard. Diagnostic ADC-based cut-off values for discrimination of the three tumor groups were chosen to yield the highest possible specificity while maintaining a clinically acceptable sensitivity.

Results. ADC values of pre-malignant ANFs clustered between BPNSTs and MPNSTs. Best BPNST vs. ANF + MPNST discrimination was obtained using ADC_{dark} at a cut-off value of 1.6×10^{-3} mm^2/s (85.3% sensitivity, 93.3% specificity), corresponding to an AUC of 94.3% (95% confidence interval: 85.2–98.0). Regarding BPNST + ANF vs. MPNST, best discrimination was obtained using an ADC_{dark} cut-off value of 1.4×10^{-3} mm^2/s (83.3% sensitivity, 94.5% specificity).

Conclusions. DW-MRI using ADC_{dark} allows specific and noninvasive discrimination of benign, atypical, and malignant nerve sheath tumors in NF1.

Key Points

- Malignant transformation of nerve sheath tumors is an important cause of death in NF1.
- Diffusion-weighted MRI using the ADC separates benign from atypical and malignant tumors.
- The ADC is a noninvasive marker for malignant transformation of nerve sheath tumors.

Importance of the Study

Atypical neurofibromas (ANFs) are considered pre-malignant precursor lesions to malignant peripheral nerve sheath tumors (MPNSTs) in patients with neurofibromatosis type 1. Unlike MPNSTs, ANFs do not show local recurrence after previous resection nor the ability to metastasize. MPNSTs have a dismal prognosis due to their high resistance to chemotherapy and tendency to metastasize at an early stage. Therefore, specific, and ideally noninvasive techniques are needed for early detection of such a transformation process. Diffusion-weighted magnetic resonance imaging (DW-MRI) is a user-independent noninvasive functional imaging technique. DW-MRI has shown promise in discriminating benign from malignant nerve sheath tumors in NF1 patients. We therefore evaluated the utility of DW-MRI for the discrimination of benign, atypical, and malignant peripheral nerve sheath tumors. In summary, the use of diffusion-weighted MRI allows to specifically discriminate benign from atypical and malignant nerve sheath tumors, both of which require further diagnostic workup such as FDG-PET/CT or biopsy.

Neurofibromatosis type 1 (NF1) is an autosomal-dominantly inherited disorder caused by a mutation of the cell growth regulating protein neurofibromin in the NF1 gene at 17q11.2.[1] NF1 is one of the most common hereditary neurocutaneous diseases with an estimated incidence of 1:2500–1:3000.[2,3]

Development of benign peripheral nerve sheath tumors (BPNSTs) is a typical feature of NF1. BPNSTs can either appear as discrete nodules along the peripheral nerves or grow to large sizes across multiple nerve fascicles presenting as bulging and deforming plexiform neurofibromas typically located in the deep soft tissues.[4] Plexiform neurofibromas affect about 30–60% of NF1 patients and can cause pain and neurological dysfunction.[5–7] Plexiform neurofibromas are of particular clinical significance due to their inherent risk of malignant transformation.[8] Transformation to malignant peripheral nerve sheath tumors (MPNSTs) is observed in 8–16% of NF1 patients and is a major cause of mortality.[6,9] Since MPNST are highly resistant to chemotherapy and metastasize at an early stage, early detection and resection are of critical importance for treatment success.[10]

Of note, MPNSTs primarily arise from pre-malignant precursor lesions, so-called atypical neurofibromas (ANFs).[11] ANFs typically present as distinct nodular lesions and are histopathologically considered pre-malignant tumors. Unlike MPNSTs, ANFs do not show recurrence after previous resection nor the ability to metastasize.[11,12] Therefore, early detection of transformation processes from BPNST to pre-malignant ANF or MPNST is crucial for patient outcome. Especially differentiation of BPNST vs. ANF/MPNST is of clinical relevance as suspicion of ANF/MPNST results in biopsy/resection.[13]

Magnetic resonance imaging (MRI) is the imaging modality of choice for monitoring plexiform neurofibromas due to its non-invasiveness and excellent soft tissue contrast.[14] Evaluation of MRI-based features has shown promise in detecting malignant transformation.[15] Therefore, MRI evaluation of plexiform neurofibromas includes a screening for "worrisome features" suggestive of malignant transformation, including irregular tumor margins, peritumoral edema, lobulated appearance, or intratumoral heterogeneity (i.e. hemorrhages or cystic changes).[15–18] However, potential disadvantages of using qualitative imaging features include limited reproducibility among readers and limited diagnostic accuracy.[15]

Diffusion-weighted MRI (DW-MRI) is considered a useful functional MRI technique that can be applied in routine clinical practice, particularly for evaluation of acute cerebral ischemia or for the characterization of (neuro-) oncological tumor entities.[19–21] DW-MRI allows to visualize the Brownian motion of molecules in human tissue.[22] Malignant processes are often associated with tissue changes such as increased vascularization, altered mitotic activity and consecutive hypercellularity. The influence of such changes on the diffusivity of water molecules in tissues can be quantified using DW-MRI with the apparent diffusion coefficient (ADC) being the most established model in clinical routine.[23]

DW-MRI has been evaluated to discriminate MPNSTs from BPNSTs. In particular, the use of the ADC value has been proposed as an imaging biomarker indicative for malignant transformation with high diagnostic accuracy. For example, using a cut-off value of $\leq 1 \times 10^{-3}$ mm^2/s for the minimum ADC (ADC_{min}) revealed high accuracy in discriminating BPNSTs from MPNSTs (100% sensitivity, 77–94% specificity).[18,24] In a study by Well et al., the diagnostic performance of the mean ADC (ADC_{mean}) and the ADC value determined in the slice with the lowest signal intensity (ADC_{dark}) showed high accuracy in discriminating BPNSTs from MPNSTs. Proposed cut-off values of 1.6×10^{-3} mm^2/s for ADC_{mean} and 1.54×10^{-3} mm^2/s for ADC_{dark}, respectively, yielded a sensitivity of 92% and a specificity of 98%.[25] Yun et al. achieved the best diagnostic accuracy for the differentiation of benign and malignant peripheral nerve sheath tumors with an ADC_{min} threshold of 0.89×10^{-3} mm^2/s and an ADC_{mean} threshold of 1.15×10^{-3} mm^2/s.[26]

Except for Ahlawat et al. who included one ANF in their statistical analysis (the ANF was considered together with the MPNST group),[24] there is no study to date evaluating the diagnostic accuracy of DW-MRI to discriminate not only MPNSTs but also ANFs from BPNSTs.

Therefore, the aim of this study was to evaluate the diagnostic accuracy of DW-MRI for the discrimination of benign, atypical, and malignant NF1-associated peripheral nerve sheath tumors. The primary hypothesis states that the area-under-the-curve (AUC) of ADC_{mean} for discrimination of BPNST versus ANF + MPNST is >80%. The second

aim was to identify clinically relevant diagnostic ADC-based cut-off values to discriminate these tumor entities.

Methods

Study Population and Study Design

This study was approved by the local ethics board (PV4691). Written informed consent was obtained from all patients. All procedures complied with the local data protection guidelines and the Declaration of Helsinki.

In all patients, the diagnosis of NF1 was confirmed by genetic testing. Consecutive recruitment was performed from 08/2014 to 12/2021. A subset of patients ($n = 26$, only BPNST and MPNSTs) was included in a previous study by Well et al.[25]

This is a prospective explorative single-center phase II diagnostic study with a paired comparative, completely crossed multiple readers and multiple cases design (MRMC) with several lesions per patient and follow-up times.

After neurological consultation, all patients initially underwent DW-MRI. Development of clinical symptoms, particularly pain, size progression of the tumor, and presence of "worrisome features" on MRI were considered indicators for a malignant transformation. Patients who underwent primary DW-MRI were still examined by an additional FDG-PET/CT if the presence of an MPNST was suspected. Patients without suspected MPNST did not undergo additional FDG-PET/CT imaging or histopathological evaluation. The decision to perform additional clarification by means of FDG-PET/CT or biopsy/surgery was made as an interdisciplinary board decision. Following the STARD recommendations for reporting diagnostic accuracy studies, a flow chart illustrating the participants' flow through the study is attached to Supplementary Material 1.

Histopathological evaluation after tumor resection served as the reference standard for MPNSTs and ANFs. Specimen collection was performed within two weeks of DW-MRI. Resected MPNSTs were classified according to the Fédération Nationale des Centres de Lutte Contre le Cancer (FNCLCC).[27] Neuropathological diagnosis of an ANF followed the 2021 WHO classification of tumors of the central nervous system.[28] As in a previous study, tumors were considered benign when no changes in size or appearance were present in follow-up examinations within ≥24 months.[29]

DW-MRI Image Acquisition

MR imaging was performed at 3T (Philips Ingenia, Best, The Netherlands). The detailed scanning protocol was reported previously[25] and is attached to Supplementary Material 2. The DW-MRI protocol applied to the lesions of interest used an axial respiratory-triggered spin-echo planar imaging (EPI) sequence with eleven *b*-values (0, 10, 20, 30, 50, 70, 100, 300, 400, 600, and 800 s/mm^2) and partial Fourier encoding (parallel acquisition; sense factor 2.8) with TR 2300 ms; TE 67 ms; echo train length 43; flip angle 90°; slice thickness 3 mm; intersection gap 0 mm; slices 27; matrix 124 × 122; FOV 270 × 270; SPAIR; two averages. Intravenous contrast material was not administered. The scan time of the DW-MRI was 7:30 min.

Data Analysis

DW-MRI data analysis.

DW-MRI data were processed as described previously[25] using a self-developed image-analysis framework (qMapIt)[30] running on the open-source software ImageJ.[31] Quantitative parametric maps were calculated by non-linear regression with pixelwise fitting of signal intensities over the spectrum of b-values to the corresponding model. A monoexponential function was applied for ADC determination. Two radiologists (I.R. and L.W.) independently assessed the ADC by manual contouring of the tumor margins on transverse diffusion-weighted images (*b*-value 50 s/mm^2). In larger plexiform neurofibromas, those distinct nodular lesions that showed worrisome features on T2w SPAIR MRI were contoured. The dashed lines in Figure 1 (middle row) illustrate exemplary ROI contouring. In the case of macroscopically circumscribed intratumoral hemorrhage with consecutive formation of intratumoral cysts, only the solid tumor portions were considered for ROI placement. Both readers were blinded regarding the reference standard, results of FDG-PET/CT, and further clinical information. $ADC_{mean/min}$ were assessed in the three slices with largest transverse tumor diameter. ADC_{dark} was determined in a singular slice with the visually lowest signal intensity on diffusion-weighted images (*b*-value 50 s/mm^2) considering all available slices where the tumor was depicted.

Statistical analysis.

Mean and minimum ADC values from each of the three ROIs per lesion were averaged to calculate ADC_{mean} and ADC_{min}. There were no missing values in either ADC values or the reference standard.

To evaluate diagnostic accuracy, the three-level reference standard was dichotomized in four different ways:

- Discrimination 1: BPNST vs. ANF + MPNST
- Discrimination 2: BPNST + ANF vs. MPNST
- Discrimination 3: BPNST vs. ANF
- Discrimination 4: ANF vs. MPNST

Only Discrimination 1 and 2 are relevant for clinical application as they reveal diagnostic accuracy under consideration of all three tumor groups. Moreover, they allow mutual discrimination of the three tumor groups by appropriate choice of cut-off values for clinical use. Instead, Discrimination 3 and 4 lead to hypothetical diagnostic accuracy measures assuming that either MPNSTs or BPNSTs do not occur.

The primary research hypothesis is based on Discrimination 1, equivalent to the approach of Ahlawat et al. who considered ANFs and MPNSTs together in statistical analysis due to invasive treatment of both tumor entities.[24] It states that the AUC of ADC_{mean} for the discrimination of BPNST vs. ANF + MPNST is > 80%. Further secondary analyses refer to the calculation of AUC of ADC_{mean}, ADC_{min}, and ADC_{dark} for any remaining choice of discrimination,

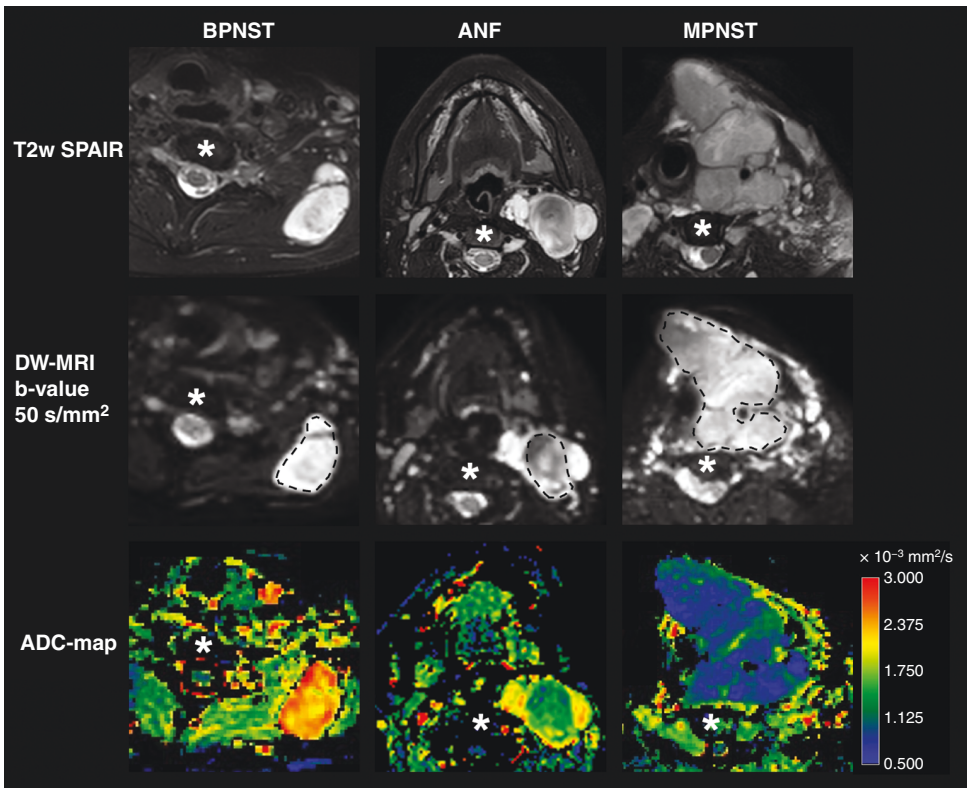

Figure 1. Exemplary assessment of DW-MRI-based ADC values in three different patients with different nerve sheath tumors of the neck. Upper row: Transverse T2-weighted SPAIR MRI (for anatomical reference purposes). Middle row: Transverse diffusion-weighted images (*b*-value 50 s/mm²). Dashed lines visualize exemplary manual ROI contouring along the tumor margins. Lower row: Corresponding parametric ADC-maps. Left: BPNST in a 39-year-old female patient. Middle: ANF in a 17-year-old male patient presenting as a distinct nodular lesion within a plexiform neurofibroma with low signal intensity on T2-weighted imaging. Right: MPNST in a 41-year-old female patient. BPNST = benign peripheral nerve sheath tumor; ANF = atypical neurofibroma; MPNST = malignant peripheral nerve sheath tumor; SPAIR = spectral attenuated inversion recovery; DW-MRI = diffusion-weighted magnetic resonance imaging.

respectively. Receiver-operating-characteristic (ROC) curves were drawn for ADC_{mean}, ADC_{min}, and ADC_{dark} based on Discrimination 1. ADC-based cut-off values were determined to discriminate between BPNSTs, ANFs, and MPNSTs based on Discrimination 1 and 2.

Statistical analysis was performed using the software R, version 4.0.5 (R Foundation for Statistical Computing, Vienna, Austria).[32] Sample size calculation is reported in Supplementary Material 3.

As there was only one primary research hypothesis, there was no need to adjust for multiplicity. The two-sided significance level was set to 5%. A non-parametric multifactorial approach was used to calculate diagnostic accuracy measures with two-sided range-preserving 95% logit transformed Wald confidence intervals (CI) averaged over both readers.[33] The primary research hypothesis was considered significant if the lower bound of the 95%-CI of the AUC of ADC_{mean} was > 80%. ROC curves were drawn based on the calculated sensitivities and specificities. Cut-off values were chosen under clinical considerations to result in the highest possible specificity with clinically acceptable sensitivity. Specificity was aimed to be as high as possible to avoid false-positive results leading to unnecessary invasive treatment in patients with benign tumors.

In detail, a baseline specificity of 80% was set. Cut-off values were then adjusted to increase specificity if no significant drop in sensitivity was seen. For each cut-off value, sensitivity, specificity, and positive and negative predictive values are reported with according two-sided 95%-CI.

To compare tumor groups, a mixed model[34] was calculated with each ADC value as the dependent variable. A random-intercept for each patient was included. Tumor group and reader were included as fixed effects. Marginal means with two-sided 95%-CI were calculated to estimate ADC values in each tumor group. Contrasts of estimated marginal means between tumor groups were calculated for pairwise comparisons. Krippendorffs alpha with bootstrapped two-sided 95%-CI and Bland–Altman plots were used to determine the agreement between the two readers.[35]

Results

Study Population and Reference Standard

Forty-nine MRI examinations were performed in 44 patients (23 male; mean age 30.1 ± 11.8 years; range 9–54 years). The resulting data set included 60 BPNSTs, 13

ANFs, and 21 MPNSTs. Histopathological reports following MPNST resection revealed 1 FNCLCC grade I, 7 grade II, and 13 grade III tumors. Considering the topographic distribution of tumors, we observed 17 tumors of the head and neck region (18%; 12 BPNSTs/ 2 ANFs/ 3 MPNSTs), 16 tumors of the thorax and thoracic wall (17%; 9 BPNSTs/ 1 ANF/ 6 MPNSTs), 46 tumors of the abdomen and abdominal wall (49%; 34 BPNSTs/ 5 ANFs/ 7 MPNSTs), 13 tumors of the lower extremities (14%; 4 BPNSTs/ 5 ANFs/ 4 MPNSTs), and two of the upper extremities (2%; 1 BPNST/ 1 MPNST). Exemplary ADC-maps of a BPNST, ANF, and MPNST are shown in Figure 1 (lower row).

Distribution of ADC Parameters of BPNSTs, ANFs, and MPNSTs

Estimated marginal means and CI for the three evaluated DW-MRI-derived ADC parameters are given in Table 1A and visualized in Figure 2. Supplementary Material 4 shows results of mixed models used to estimate the marginal means for comparing ADC values between tumor groups.

Estimated marginal means for ADC_{mean} were 2.14×10^{-3} mm^2/s (95%-CI: 2.05–2.24) for BPNSTs, 1.63×10^{-3} mm^2/s (1.49–1.78) for ANFs, and 1.41×10^{-3} mm^2/s (1.29–1.53) for MPNSTs.

Regarding ADC_{min}, estimated marginal means were 1.63×10^{-3} mm^2/s (95%-CI: 1.52–1.74) for BPNSTs, 1.09×10^{-3} mm^2/s (0.91–1.26) for ANFs, and 0.82×10^{-3} mm^2/s (0.68–0.97) for MPNSTs.

Regarding ADC_{dark}, estimated marginal means were 2.07×10^{-3} mm^2/s (95%-CI: 1.98–2.16) for BPNSTs, 1.57×10^{-3} mm^2/s (1.42–1.71) for ANFs, and 1.30×10^{-3} mm^2/s (1.18–1.42) for MPNSTs.

Differences of the ADC values and *P*-values of the pairwise comparisons are displayed in Table 1B. All pairwise comparisons of BPNST vs. ANF vs. MPNST group revealed P-values < .05.

Agreement across the two readers was excellent. Krippendorffs alpha of ADC_{mean} was 0.98 (95%-CI: 0.97–0.99). For ADC_{min}, Krippendorffs alpha was 0.91 (0.82–0.97) and for ADC_{dark} it was 0.97 (0.95–0.98). In Supplementary Material 5 we provide Bland–Altmann plots for $ADC_{mean/min/dark}$ stratified by tumor type.

ROC-AUC Analysis for BPNST, ANF, and MPNST Discrimination

Separate ROC curves for the comparison BPNST vs. ANF + MPNST (Discrimination 1) using ADC_{mean}, ADC_{min}, and ADC_{dark} are shown in Figure 3.

AUC values including CI for the three ADC parameters and both discriminations are shown in Table 2. With respect to ADC_{mean}, the AUC for the comparison BPNST vs. ANF + MPNST (Discrimination 1) was 93.9% (95%-CI: 84.1–97.8). Thus, the primary research hypothesis can be confirmed since the lower limit of the 95% CI of ADC_{mean} (84.1%) is > 80%. For the same comparison, the AUC of ADC_{min} was 92.5% (95%-CI: 84.0–96.7) and the AUC of ADC_{dark} was 94.3% (85.2–98.0).

With respect to the second comparison BPNST + ANF vs. MPNST (Discrimination 2), highest AUC was obtained using ADC_{mean} (97.1% (95%-CI: 91.0–99.1)). The AUC of ADC_{min} was 96.0% (90.2–98.4) and of ADC_{dark} 96.2% (89.1–98.7).

Table 1. Estimated Marginal Means and Pairwise Comparisons for ADCmean, ADCmin, and ADCdark

(A) Estimated marginal means	ADC parameter		BPNST (*n* = 60)	ANF (*n* = 13)	MPNST (*n* = 21)
	ADC_{mean} [$\times 10^{-3}$ mm^2/s] (95%-CI)		2.14 (2.05–2.24)	1.63 (1.49–1.78)	1.41 (1.29–1.53)
	ADC_{min} [$\times 10^{-3}$ mm^2/s] (95%-CI)		1.63 (1.52–1.74)	1.09 (0.91–1.26)	0.82 (0.68–0.97)
	ADC_{dark} [$\times 10^{-3}$ mm^2/s] (95%-CI)		2.07 (1.98–2.16)	1.57 (1.42–1.71)	1.30 (1.18–1.42)
(B) Pairwise comparisons	**ADC parameter**		**BPNST vs. ANF**	**BPNST vs. MPNST**	**ANF vs. MPNST**
	ADC_{mean}	Difference [$\times 10^{-3}$ mm^2/s] (95%-CI)	0.51 (0.35–0.67)	0.73 (0.62–0.85)	0.22 (0.06–0.39)
		P-value	<.0001	<.0001	.0096
	ADC_{min}	Difference [$\times 10^{-3}$ mm^2/s] (95%-CI)	0.54 (0.35–0.73)	0.81 (0.66–0.95)	0.26 (0.06–0.47)
		P-value	<.0001	<.0001	.0137
	ADC_{dark}	Difference [$\times 10^{-3}$ mm^2/s] (95%-CI)	0.51 (0.34–0.67)	0.77 (0.64–0.90)	0.26 (0.09–0.44)
		P-value	<.0001	<.0001	.0041

ADC_{mean} = mean apparent diffusion coefficient; ADC_{min} = minimum apparent diffusion coefficient; ADC_{dark} = apparent diffusion coefficient in the slice with lowest signal intensity; BPNST = benign peripheral nerve sheath tumor; ANF = atypical neurofibroma; MPNST = malignant peripheral nerve sheath tumor; CI = confidence interval.

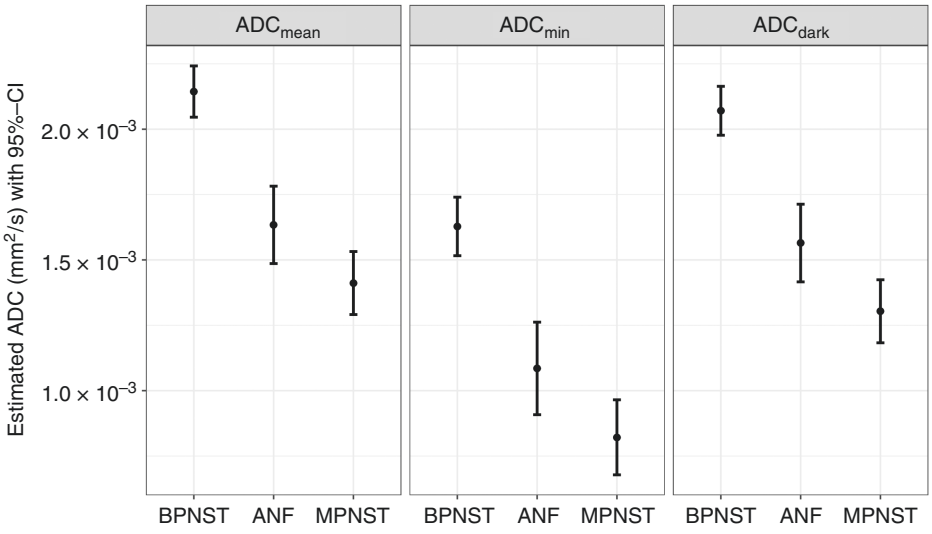

Figure 2. Estimated marginal means for ADC_{mean}, ADC_{min}, and ADC_{dark} of benign (BPNST), atypical (ANF), and malignant (MPNST) peripheral nerve sheath tumors. ADC_{mean} = mean apparent diffusion coefficient; ADC_{min} = minimum apparent diffusion coefficient; ADC_{dark} = apparent diffusion coefficient in the slice with lowest signal intensity; BPNST = benign peripheral nerve sheath tumor; ANF = atypical neurofibroma; MPNST = malignant peripheral nerve sheath tumor; CI = confidence interval.

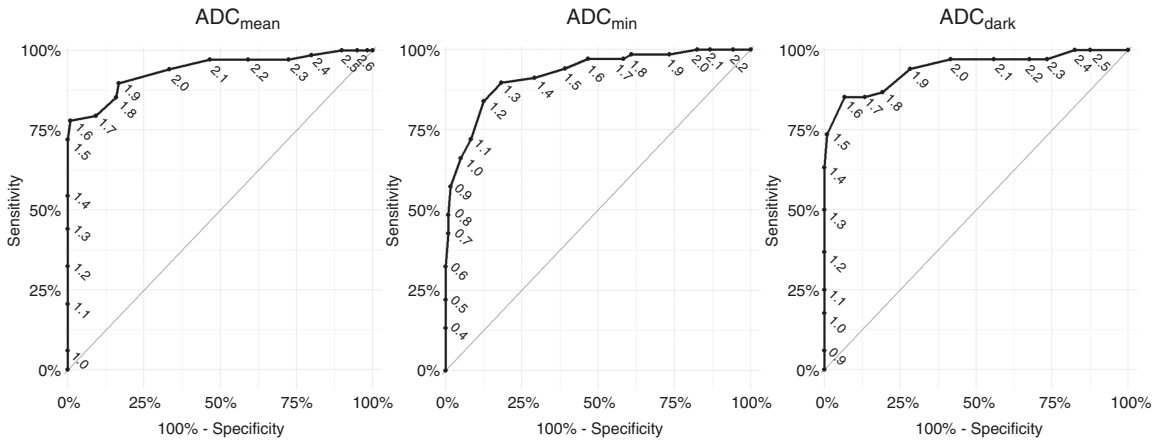

Figure 3. ROC analyses for the comparison BPNST vs. ANF + MPNST using ADC_{mean}, ADC_{min}, and ADC_{dark}. Oblique numbers along the curves correspond to potential cut-off values × 10^{-3}mm²/s. ADC_{mean} = mean apparent diffusion coefficient; ADC_{min} = minimum apparent diffusion coefficient; ADC_{dark} = apparent diffusion coefficient in the slice with lowest signal intensity.

Definition of Optimal Cut-off Values for Tumor Discrimination

The highest specificity combined with a clinically acceptable sensitivity for the discrimination of BPNST vs. ANF + MPNST (Discrimination 1) was obtained with ADC_{dark} using a cut-off value of 1.6 × 10^{-3} mm²/s, resulting in a sensitivity of 85.3% and specificity of 93.3%. For the discrimination of BPNST + ANF vs. MPNST (Discrimination 2) by ADC_{dark}, a cut-off value of 1.4 × 10^{-3} mm²/s resulted in a sensitivity of 83.3% and a specificity of 94.5% (Table 2).

Regarding ADC_{mean}, discrimination of BPNST vs. ANF + MPNST (Discrimination 1) using the same cut-off value of 1.6 × 10^{-3} mm²/s revealed a sensitivity of 77.9% and a specificity of 99.2%. Discrimination of BPNST + ANF vs. MPNST (Discrimination 2) using a cut-off value of 1.4 × 10^{-3} mm²/s resulted in a sensitivity of 78.6% and a specificity of 97.3%.

ADC_{min} yielded the lowest sensitivity: Using a cut-off value of 1.1 × 10^{-3} mm²/s for discrimination of BPNST vs. ANF + MPNST (Discrimination 1) corresponded to a sensitivity of 72.1% and a specificity of 91.7%. For the discrimination of BPNST + ANF vs. MPNST (Discrimination 2), a sensitivity of 81.0% and a specificity of 95.2% was achieved using a cut-off value of 0.9 × 10^{-3} mm²/s.

A comprehensive overview including all potential ADC-based cut-off values for both discriminations is

Table 2. ROC-Analyses-Derived AUC Values for ADC_{mean}, ADC_{min}, and ADC_{dark} and Choice of Appropriate Cut-off Values

Comparison	ADC parameter	AUC [%] (95%-CI)	Cut-off value [$\times 10^{-3}$ mm^2/s]	Sensitivity [%] (95%-CI)	Specificity [%] (95%-CI)	PPV [%] (95%-CI)	NPV [%] (95%-CI)
BPNST vs. ANF + MPNST	ADC_{mean}	93.9 (84.1–97.8)	1.6	77.9 (59.3–89.6)	99.2	98.2	88.8 (79.8–94.1)
	ADC_{min}	92.5 (84.0–96.7)	1.1	72.1 (55.1–84.4)	91.7 (85.2–95.5)	83.1 (67.5–92.0)	85.3 (74.9–91.8)
	ADC_{dark}	94.3 (85.2–98.0)	1.6	85.3 (67.8–94.1)	93.3 (82.3–97.7)	88.0 (74.8–94.7)	91.8 (82.5–96.4)
BPNST + ANF vs. MPNST	ADC_{mean}	97.1 (91.0–99.1)	1.4	78.6 (58.3–90.6)	97.3 (89.2–99.4)	89.2 (49.9–98.6)	94.0 (88.0–97.2)
	ADC_{min}	96.0 (90.2–98.4)	0.9	81.0 (62.1–91.7)	95.2 (87.7–98.2)	83.0 (52.5–95.6)	94.6 (88.4–97.5)
	ADC_{dark}	96.2 (89.1–98.7)	1.4	83.3 (61.8–93.9)	94.5 (86.7–97.9)	81.4 (48.3–95.3)	95.1 (88.9–98.0)

ADC_{mean} = mean apparent diffusion coefficient; ADC_{min} = minimum apparent diffusion coefficient; ADC_{dark} = apparent diffusion coefficient in the slice with lowest signal intensity; ANF = atypical neurofibroma; AUC = area-under-the-curve; BPNST = benign peripheral nerve sheath tumor; CI = confidence interval; MPNST = malignant peripheral nerve sheath tumor; PPV = positive predictive value; NPV = negative predictive value; ROC = receiver-operating characteristic.

included in Supplementary Material 6. Hypothetical cut-off values assuming either MPNSTs or BPNSTs do not occur (i.e. BPNST vs. ANF, ANF vs. MPNST) are reported in Supplementary Material 7. The numbers of categorized tumors based on the determined cut-off values are visualized in Supplementary Material 8 using cross tabulations.

Discussion

In this study, we demonstrated the utility of DW-MRI to discriminate benign, atypical, and malignant NF1-associated peripheral nerve sheath tumors. ADC values of atypical tumors clustered between benign and malignant peripheral nerve sheath tumors, according to their histopathological classification as pre-malignant tumors. Compared to mean and minimum ADC, ADC assessed in the slice of a given tumor with lowest signal intensity (ADC_{dark}) yielded best diagnostic accuracy, corresponding to an AUC of 94.3%. We therefore propose the use of ADC_{dark} for evaluation of NF1-associated peripheral nerve sheath tumors. In our patient collective, ADC_{dark}-derived cut-off values of 1.6×10^{-3} mm^2/s for discrimination of BPNST vs. ANF + MPNST and of 1.4×10^{-3} mm^2/s for discrimination of BPNST + ANF vs. MPNST yielded the most favorable results with high specificity while maintaining a clinically satisfactory sensitivity.

When interpreting the reported sensitivities (72.1%–85.3%), it should be considered that some of the results have quite wide 95%-CI. However, when compared with other reported studies and especially meta-analytic workups, this appears to be a general observation in the assessment of diagnostic tools for the classification of NF1-associated tumors.[15] Therefore, the reported sensitivities could also be interpreted against the background of the disease, i.e. representing a diagnostic limitation associated with NF1 due to tumor heterogeneity.[36]

Contrary to Demehri et al.[18] and Ahlawat et al.,[24,37] but in line with Yun et al.[26] the diagnostic performance of ADC_{min} was slightly lower when compared to ADC_{mean}. Our proposed cut-off values resulted in a sensitivity of less than 100%, which has been reported by Ahlawat et al.[24,37] We aimed to achieve a reasonably high specificity to reduce the risk of false-positive results, which might lead to unnecessary, potentially mutilating surgery of affected patients. However, these prior studies performed the evaluation of their diagnostic accuracy under consideration of only two groups (BPNST vs. MPNST). The slightly lower sensitivities in our study should therefore be evaluated against the background that ANFs were included as a third and independent tumor entity in our study. ADC values of the ANFs clustered between BPNST and MPNST, indicating biological plausibility, but making it more difficult to clearly distinguish these three tumor entities.

The use of DW-MRI-based quantitative parameters allows a more specific diagnosis of malignant transformation compared to using only morphological MRI criteria.[15] Although promising sensitivities have been reported with respect to the use of MRI-based morphologic criteria to discriminate BPNSTs from MPNSTs, these criteria are often not very specific. For example, using the criterion "loss of the target sign" revealed a high pooled sensitivity of 99% but a comparably low pooled specificity of only 33% in a recent meta-analysis.[15] According to the meta-analysis by Martin et al., only the criterion "tumor size" seems to be reasonably comparable to DW-MRI in its diagnostic performance with a sufficient specificity of 85% and a sensitivity of 71%.[15]

The study has the following limitations: First, the number of MPNSTs and ANFs is relatively small, which is explicable by the rarity of the disease. Nevertheless, the sample size is comparable with existing studies.[18,24–26,37]

Second, intervendor and intersystem variability of ADC measurements limit the generalizability of the proposed cut-off values. Although previous studies have shown

only minor differences, any variations in technical equipment and imaging protocol (e.g. the use of fewer *b*-values) should be considered in the context of the results derived from our single-center study.[38,39] One way to address this limitation in the future would be to conduct multicenter studies, which may allow the identification of generalizable parameters with clinically appropriate cut-off values that can be robustly reproduced across different sites independent of site-specific acquisition parameters.

Third, the ADC-based cut-off values were selected in a data-driven manner, potentially overestimating diagnostic accuracy.[40] Future validation in an independent cohort is needed to address this potential overestimation.

Furthermore, future studies need to investigate whether the diagnostic performance of the more available, less costly, and noninvasive DW-MRI is noninferior to the FDG-PET/CT for the discrimination of BPNSTs, ANFs, and MPNSTs.

To conclude, DW-MRI using ADC_{dark} allows specific and noninvasive discrimination of benign from atypical and malignant peripheral nerve sheath tumors in NF1.

Supplementary material

Supplementary material is available online at *Neuro-Oncology* (https://academic.oup.com/neuro-oncology).

Keywords

apparent diffusion coefficient | DWI | MRI | malignant peripheral nerve sheath tumor | neurofibromatosis type 1

Funding

I.R. and J.S. were supported by a research grant from the German lay organization "Bundesverband Neurofibromatose e.V." (grant no. n/a). Further funding was provided to L.W. and J.S. by the "Werner-Otto-Stiftung" (grant no. 13/97). The funders had no role in study design, data collection and analysis, decision to publish, or preparation of the manuscript. M.G.K., M.S., A.Z., C.R., A.L., V.F.M., S.F., I.A., G.A., and P.B. report no disclosures relevant to the manuscript.

Conflict of interest statement

The authors report no conflict of interest. All authors have approved the final version of the article.

Authorship statement

Study conception: J.S., L.W. Planning of imaging sequences: J.S., L.W. DW-MRI data acquisition: I.R., J.S., L.W., C.R., A.L. Data and statistical analysis: I.R., L.W., I.A., M.K., M.S., A.Z. Manuscript drafting: I.R., L.W. Contribution in writing and revising the manuscript: J.S., M.S., A.Z., I.A., M.K., C.R., A.L., G.A., P.B., S.F., V.F.M.

Affiliations

Department of Diagnostic and Interventional Radiology and Nuclear Medicine, University Medical Center Hamburg-Eppendorf, Hamburg, Germany (I.R., M.G.K., C.R., A.L., I.A., G.A., P.B., J.S., L.W.); Institute of Medical Biometry and Epidemiology, University Medical Center Hamburg-Eppendorf, Hamburg, Germany (M.S., A.Z.); Department of Neurology, University Medical Center Hamburg-Eppendorf, Hamburg, Germany (V.F.M., S.F.); Department of Diagnostic and Interventional Radiology, Medical Care Center Beste Trave, Bad Oldesloe, Germany (J.S.)

References

1. Viskochil D. Genetics of neurofibromatosis 1 and the NF1 gene. *J Child Neurol*. 2002;17(8):562–570; discussion 571.
2. Lammert M, Friedman JM, Kluwe L, Mautner VF. Prevalence of neurofibromatosis 1 in german children at elementary school enrollment. *Arch Dermatol*. 2005;141(1):71–74.
3. Huson SM, Compston DA, Harper PS. A genetic study of von Recklinghausen neurofibromatosis in south east Wales. II. Guidelines for genetic counselling. *J Med Genet*. 1989;26(11):712–721.
4. Korf BR. Plexiform neurofibromas. *Am J Med Genet*. 1999;89(1):31–37.
5. Seminog OO, Goldacre MJ. Risk of benign tumours of nervous system, and of malignant neoplasms, in people with neurofibromatosis: population-based record-linkage study. *Br J Cancer*. 2013;108(1):193–198.
6. Evans DGR, Baser ME, McGaughran J, et al. Malignant peripheral nerve sheath tumours in neurofibromatosis. *J Med Genet*. 2002;39(5):311–314.
7. Mautner VF, Asuagbor FA, Dombi E, et al. Assessment of benign tumor burden by whole-body MRI in patients with neurofibromatosis 1. *Neuro Oncol*. 2008;10(4):593–598.
8. Tucker T, Wolkenstein P, Revuz J, Zeller J, Friedman JM. Association between benign and malignant peripheral nerve sheath tumors in NF1. *Neurology*. 2005;65(2):205–211.
9. Uusitalo E, Rantanen M, Kallionpää RA, et al. Distinctive cancer associations in patients with neurofibromatosis type 1. *J Clin Oncol*. 2016;34(17):1978–1986.
10. Ducatman BS, Scheithauer BW, Piepgras DG, Reiman HM, Ilstrup DM. Malignant peripheral nerve sheath tumors a clinicopathologic study of 120 cases. *Cancer*. 1986;57(10):2006–2021.
11. Miettinen MM, Antonescu CR, Fletcher CDM, et al. Histopathologic evaluation of atypical neurofibromatous tumors and their transformation into malignant peripheral nerve sheath tumor in patients with neurofibromatosis 1—a consensus overview. *Hum Pathol*. 2017;67:1–10.
12. Beert E, Brems H, Daniëls B, et al. Atypical neurofibromas in neurofibromatosis type 1 are premalignant tumors. *Genes Chromosomes Cancer*. 2011;50(12):1021–1032.
13. Gronchi A, Miah AB, Dei Tos AP, et al; ESMO Guidelines Committee, EURACAN and GENTURIS. Electronic address: clinicalguidelines@esmo.org. ESMO Guidelines Committee, EURACAN and GENTURIS: Soft tissue and visceral sarcomas: ESMO-EURACAN-GENTURIS Clinical

Practice Guidelines for diagnosis, treatment and follow-up☆. *Ann Oncol*. 2021;32(11):1348–1365.

14. Ahlaw at S, Blakeley JO, Langmead S, Belzberg AJ, Fayad LM. Current status and recommendations for imaging in neurofibromatosis type 1, neurofibromatosis type 2, and schwannomatosis. *Skeletal Radiol*. 2020;49(2):199–219.
15. Martin E, Geitenbeek RTJ, Coert JH, et al. A Bayesian approach for diagnostic accuracy of malignant peripheral nerve sheath tumors: a systematic review and meta-analysis. *Neuro Oncol*. 2021;23(4):557–571.
16. Wasa J, Nishida Y, Tsukushi S, et al. MRI features in the differentiation of malignant peripheral nerve sheath tumors and neurofibromas. *AJR Am J Roentgenol*. 2012;194(6):1568–1574.
17. Matsumine A, Kusuzaki K, Nakamura T, et al. Differentiation between neurofibromas and malignant peripheral nerve sheath tumors in neurofibromatosis 1 evaluated by MRI. *J Cancer Res Clin Oncol*. 2009;135(7):891–900.
18. Demehri S, Belzberg A, Blakeley J, Fayad LM. Conventional and functional MR imaging of peripheral nerve sheath tumors: initial experience. *AJNR Am J Neuroradiol*. 2014;35(8):1615–1620.
19. Charles-Edwards EM, deSouza NM. Diffusion-weighted magnetic resonance imaging and its application to cancer. *Cancer Imaging*. 2006;6(1):135–143.
20. Lee SY, Jee WH, Jung JY, et al. Differentiation of malignant from benign soft tissue tumours: use of additive qualitative and quantitative diffusion-weighted MR imaging to standard MR imaging at 3.0 T. *Eur Radiol*. 2016;26(3):743–754.
21. Albers GW. Diffusion-weighted MRI for evaluation of acute stroke. *Neurology*. 1998;51(3 Suppl 3):S47–S49.
22. Baliyan V, Das CJ, Sharma R, Gupta AK. Diffusion weighted imaging: technique and applications. *World J Radiol*. 2016;8(9):785–798.
23. Tang L, Zhou XJ. Diffusion MRI of cancer: from low to high b-values. *J Magn Reson Imaging*. 2019;49(1):23–40.
24. Ahlawat S, Blakeley JO, Rodriguez FJ, Fayad LM. Imaging biomarkers for malignant peripheral nerve sheath tumors in neurofibromatosis type 1. *Neurology*. 2019;93(11):e1076–e1084.
25. Well L, Salamon J, Kaul MG, et al. Differentiation of peripheral nerve sheath tumors in patients with neurofibromatosis type 1 using diffusion-weighted magnetic resonance imaging. *Neuro Oncol*. 2019;21(4):508–516.
26. Yun JS, Lee MH, Lee SM, et al. Peripheral nerve sheath tumor: differentiation of malignant from benign tumors with conventional and diffusion-weighted MRI. *Eur Radiol*. 2021;31(3):1548–1557.
27. Trojani M, Contesso G, Coindre JM, et al. Soft-tissue sarcomas of adults; study of pathological prognostic variables and definition of a histopathological grading system. *Int J Cancer*. 1984;33(1):37–42.
28. Louis DN, Perry A, Wesseling P, et al. The 2021 WHO classification of tumors of the central nervous system: a summary. *Neuro Oncol*. 2021;23(8):1231–1251.
29. Ristow I, Madesta F, Well L, et al. Evaluation of MRI-based radiomics characteristics for differentiation of benign and malignant peripheral nerve sheath tumors in neurofibromatosis type 1. *Neuro Oncol*. 2022;24(10):1790–1798.
30. Herrmann J, Ittrich H, Kaul MG, et al. Functional assessment of the kidneys in a 10 month-old child with renal artery stenosis by intravoxel incoherent motion. *Nephrology*. 2017;22(3):257–260.
31. Schneider CA, Rasband WS, Eliceiri KW. NIH image to ImageJ: 25 years of image analysis. *Nat Methods*. 2012;9(7):671–675.
32. R Core Team. R: A language and environment for statistical computing. 2021. Vienna, Austria: R Foundation for Statistical Computing. URL https://www.R-project.org/
33. Brunner E, Zapf A. Nonparametric ROC analysis for diagnostic trials. *Methods Appl Stat Clin Trials: Plan, Anal Inferent Meth*. 2014;2:483–495.
34. Kuznetsova A, Brockhoff PB, Christensen RHB. lmertest package: tests in linear mixed effects models. *J Stat Softw*. 2017;82(13):1–26.
35. Hughes J. krippendorffsalpha: An R Package for Measuring Agreement Using Krippendorff's Alpha Coefficient. R package version 1.1-1. 2021. https://CRAN.R-project.org/package=krippendorffsalpha
36. Carrió M, Gel B, Terribas E, et al. Analysis of intratumor heterogeneity in Neurofibromatosis type 1 plexiform neurofibromas and neurofibromas with atypical features: correlating histological and genomic findings. *Hum Mutat*. 2018;39(8):1112–1125.
37. Ahlawat S, Fayad LM. Imaging cellularity in benign and malignant peripheral nerve sheath tumors: utility of the "target sign" by diffusion weighted imaging. *Eur J Radiol*. 2018;102:195–201.
38. Keenan KE, Delfino JG, Jordanova KV, et al. Challenges in ensuring the generalizability of image quantitation methods for MRI. *Med Phys*. 2022;49(4):2820–2835.
39. Donati OF, Chong D, Nanz D, et al. Diffusion-weighted MR imaging of upper abdominal organs: field strength and intervendor variability of apparent diffusion coefficients. *Radiology*. 2014;270(2):454–463.
40. Leeflang MMG, Moons KGM, Reitsma JB, Zwinderman AH. Bias in sensitivity and specificity caused by data-driven selection of optimal cutoff values: mechanisms, magnitude, and solutions. *Clin Chem*. 2008;54(4):729–737.